

# Path Integral Formulation of Stochastic Optimal Control with Generalized Costs<sup>\*</sup>

Insoon Yang<sup>\*</sup> Matthias Morzfeld<sup>\*\*</sup> Claire J. Tomlin<sup>\*</sup>  
Alexandre J. Chorin<sup>\*\*</sup>

<sup>\*</sup> *Department of Electrical Engineering and Computer Sciences,  
University of California, Berkeley, CA 94720 USA (e-mail:  
iyang@eecs.berkeley.edu, tomlin@eecs.berkeley.edu)*

<sup>\*\*</sup> *Department of Mathematics, University of California, Berkeley and  
Lawrence Berkeley National Laboratory, CA 94720 USA (e-mail:  
mmo@math.lbl.gov, chorin@math.berkeley.edu)*

---

**Abstract:** Path integral control solves a class of stochastic optimal control problems with a Monte Carlo (MC) method for an associated Hamilton-Jacobi-Bellman (HJB) equation. The MC approach avoids the need for a global grid of the domain of the HJB equation and, therefore, path integral control is in principle applicable to control problems of moderate to large dimension. The class of problems path integral control can solve, however, is defined by requirements on the cost function, the noise covariance matrix and the control input matrix. We relax the requirements on the cost function by introducing a new state that represents an augmented running cost. In our new formulation the cost function can contain stochastic integral terms and linear control costs, which are important in applications in engineering, economics and finance. We find an efficient numerical implementation of our grid-free MC approach and demonstrate its performance and usefulness in examples from hierarchical electric load management. The dimension of one of our examples is large enough to make classical grid-based HJB solvers impractical.

---

## 1. INTRODUCTION

Stochastic optimal control is an important tool for controlling or analyzing stochastic systems in many fields, including engineering, economics and finance. In electric power systems, for example, uncertainties from renewable energy sources can be managed using stochastic optimal control techniques (e.g. Anderson et al. [2011], Yang et al. [2014]).

A popular method for stochastic optimal control is to compute an optimal feedback map from the system state to the control via dynamic programming (Bellman [1956]). For systems modeled by stochastic differential equations (SDEs), dynamic programming leads to a Hamilton-Jacobi-Bellman (HJB) equation, whose viscosity solution corresponds to the value function of the stochastic optimal control problem (Fleming and Soner [2005]). An optimal control strategy can be synthesized from information about the value function.

The complexity and memory requirements of grid-based partial differential equation (PDE) solvers increase exponentially as the dimension of the system increases. This makes grid-based methods impractical for problems of large dimension. As an alternative to grid-based PDE solvers one can use Monte Carlo (MC) schemes. This

is the main idea in “path integral control” (Kappen [2005a,b], Todorov [2009], Theodorou et al. [2010, 2011], Morzfeld [2013]), which use the Feynman-Kac formula (see e.g. Chorin and Hald [2013]), i.e. a path integral, to solve a class of HJB equations. The current theory of path integral control requires several assumptions about the cost function, noise covariance and control input matrices. These assumptions are often restrictive and can prevent its broad application. A related method that can help with the scaling of grid-based PDE solvers is the “max-plus” method (McEneaney et al. [2008], McEneaney and Kluberg [2009]).

Our goal is to extend path integral control to handle more general cost functions, in particular costs involving stochastic (Itô) integral terms or linear control costs. Cost functions with stochastic integral terms are important in dynamic contract problems where one needs to incorporate the risk aversions of a principal and an agent into the contract (e.g. Holmstrom and Milgrom [1987]); linear terms in the control cost are important in hierarchical electric load management problems (see Section 4). We introduce a new state variable that integrates the running costs from the initial time to the current time. We then use dynamic programming to derive the HJB equation associated with the control problem in the augmented state space. We can use the Feynman-Kac formula to solve the HJB equation because we do not introduce any additional requirements on the control input matrix or noise covariance matrix. Thus, we can solve control problems with generalized costs using the path integral-based method.

---

<sup>\*</sup> This work was supported by the NSF CPS project ActionWebs under grant number 0931843, NSF CPS project FORCES under grant number 1239166, by the Director, Office of Science, Computational and Technology Research, U.S. Department of Energy under Contract No. DE-AC02-05CH11231, and by the National Science Foundation under grant DMS-1217065.

We use implicit sampling (Chorin and Tu [2009], Chorin et al. [2010], Morzfeld et al. [2012], Morzfeld and Chorin [2012], Atkins et al. [2013], Morzfeld [2013]) to evaluate the Feynman-Kac formula numerically. Implicit sampling is an MC sampling scheme that guides the samples to high-probability regions via a numerical optimization. This can be particularly advantageous (compared to traditional MC sampling) if the running cost has deep wells (Kappen [2005a], Morzfeld [2013]).

The efficiency and usefulness of our approach is demonstrated with an example from hierarchical management of groups of thermostatically controlled loads (TCLs). The dimension of the state space of this example is large enough to make grid based PDE solvers impractical.

The remainder of this paper is organized as follows. In Section 2, we review path integral control and its limitations. We explain our generalization in Section 3 and also discuss our implementation with implicit sampling. In Section 4 we apply our method to a problem in direct load control.

## 2. REVIEW OF PATH INTEGRAL CONTROL

Consider a process  $\{x_t\}_{0 \leq t \leq T}$ ,  $x_t \in \mathbb{R}^n$  that is driven by the stochastic differential equation (SDE):

$$\begin{aligned} dx_t &= [f(t, x_t) + Ku_t]dt + \sigma dW_t \\ x_0 &= x^0, \end{aligned} \quad (1)$$

where  $K \in \mathbb{R}^{n \times m}$  and  $\sigma \in \mathbb{R}^{n \times n}$ , and  $\{u_t\}_{0 \leq t \leq T}$ ,  $u_t \in \mathbb{R}^m$  is the control process;  $\{W_t\}_{t \geq 0}$  is an  $n$ -dimensional Brownian motion on a suitable probability space.

Path integral control requires a cost function of the form

$$\min_{u \in \mathbb{U}} \mathbb{E} \left[ \Phi(x_T) + \int_0^T V(t, x_t)dt + \frac{1}{2} \int_0^T u_t^\top Ru_t dt \right] \quad (2)$$

where  $\mathbb{U}$  is the set of feasible controls,  $R \in \mathbb{R}^{m \times m}$  is a given positive definite matrix and  $\Phi(x_T)$  and  $V(t, x_t)$  are the terminal and running costs, respectively (Kappen [2005a], Theodorou et al. [2010]); the expected value is taken over trajectories of (1).

Path integral control further requires that there exists a constant  $\lambda$  such that

$$\sigma\sigma^\top = \lambda KR^{-1}K^\top. \quad (3)$$

This condition implies that the control input through a subsystem (or a channel) with a higher noise variance is cheaper than that through a subsystem with a lower noise variance (Kappen [2005a]).

Dynamic programming can be used to derive the HJB equation for a stochastic optimal control problem. This HJB equation is generally nonlinear, however for the class of problems defined by (2) and (3), a log-transformation can be used to derive a linear HJB equation (Kappen [2005a]). The solution of this linear HJB equation can be found via the Feynman-Kac formula (a path integral).

In computations, one discretizes the path to obtain a convergent approximation of the Feynman-Kac formula. MC sampling can be used to evaluate this discretized path integral numerically and, thus, to find the solution of the HJB equation. Specifically, MC schemes evaluate a solution of

the HJB equation locally without requiring the solution nearby, so that there is no need for a (global) grid of the domain. This feature makes path integral control with MC sampling particularly effective and memory efficient when applicable.

## 3. PATH INTEGRAL FORMULATION OF STOCHASTIC OPTIMAL CONTROL WITH GENERALIZED COSTS

Our goal is to develop a path integral method that can handle cost functions that are more general than (2). Specifically, consider a stochastic optimal control problem of the form

$$\min_{u \in \mathbb{U}} \mathbb{E} \left[ \Phi \left( x_T, \int_0^T V(t, x_t)dt + \int_0^T c(t)dx_t \right) + \frac{1}{2} \int_0^T u_t^\top Ru_t dt \right], \quad (4)$$

where  $\Phi : \mathbb{R}^n \times \mathbb{R} \rightarrow \mathbb{R}$  is a given function, and where  $V(t, x_t) \in \mathbb{R}$  and  $c(t) \in \mathbb{R}^{1 \times n}$  are the running costs, the latter being the running cost associated with a stochastic state trajectory. This generalized cost function has been used in dynamic incentive design problems to take into account the principal's and the agent's risk aversions (Holmstrom and Milgrom [1987], Ou-Yang [2003]). We will further show that the generalized cost function can include running costs that are linear in the control and discuss its usefulness in hierarchical management for thermostatically controlled loads (in Section 4).

### 3.1 The augmented system

We reformulate the stochastic optimal control problem with generalized cost (4) to a related problem for which we can derive the associated HJB equation. The key idea is to introduce the new state variable

$$y_t := \int_0^t V(s, x_s)ds + \int_0^t c(s)dx_s, \quad (5)$$

where the stochastic integral is in the Itô sense. Then, the process  $\{y_t\}_{0 \leq t \leq T}$  is driven by the following SDE:

$$\begin{aligned} dy_t &= [V(t, x_t) + c(t)(f(t, x_t) + Ku_t)]dt + c(t)\sigma dW_t \\ y_0 &= 0, \end{aligned} \quad (6)$$

where  $\{W_t\}_{t \geq 0}$  is the Brownian motion in (1). We can define an augmented state space by  $(x_t, y_t)$ . The stochastic optimal control problem (4) can be rewritten in this augmented state space as

$$\min_{u \in \mathbb{U}} \mathbb{E} \left[ \Phi(x_T, y_T) + \frac{1}{2} \int_0^T u_t^\top Ru_t dt \right] \quad (7)$$

where the expectation is over the trajectories of (1) and (6).

### 3.2 The HJB equation of the augmented system

We will now provide the details about the derivation of the HJB equation for the augmented state space problem. This will highlight that path integral control can be applied to problems with generalized costs (4) provided that (3) holds, while no additional restrictions are required.

We define the value function of the stochastic optimal control as

$$\phi(\mathbf{x}, \mathbf{y}, t) := \min_{u \in \mathbb{U}} \mathbb{E}_{\mathbf{x}, \mathbf{y}, t} \left[ \Phi(x_T, y_T) + \frac{1}{2} \int_t^T u_s^\top R u_s ds \right], \quad (8)$$

where the expected values is taken over trajectories of (1) and (6) starting at  $(x_t, y_t) = (\mathbf{x}, \mathbf{y})$ . Let

$$\Lambda(t) := \begin{bmatrix} \mathbf{I}_n \\ c(t) \end{bmatrix} \in \mathbb{R}^{(n+1) \times n},$$

where  $\mathbf{I}_n$  denotes the  $n \times n$  identity matrix, and  $\hat{\sigma}(t) := \Lambda(t)\sigma$ . Dynamic programming gives the HJB equation

$$\begin{aligned} \phi_t + \min_{a \in \mathbb{R}^m} \left\{ \frac{1}{2} \text{tr}(\hat{\sigma} \hat{\sigma}^\top D^2 \phi) + (f(t, \mathbf{x}) + Ka)^\top D_{\mathbf{x}} \phi \right. \\ \left. + (V(t, \mathbf{x}) + c(t)f(t, \mathbf{x}) + c(t)Ka) D_{\mathbf{y}} \phi + \frac{1}{2} a^\top Ra \right\} = 0 \\ \phi(\mathbf{x}, \mathbf{y}, T) = \Phi(\mathbf{x}, \mathbf{y}). \end{aligned} \quad (9)$$

The minimizer in (9) is given by

$$a^* = -R^{-1} \hat{K}(t)^\top D \phi, \quad (10)$$

where  $\hat{K}(t) = \Lambda(t)K$  and  $D\phi := (D_{\mathbf{x}}\phi, D_{\mathbf{y}}\phi) \in \mathbb{R}^{n+1}$ . Plugging this minimizer into (9), we obtain

$$\begin{aligned} \phi_t + \frac{1}{2} \text{tr}(\hat{\sigma} \hat{\sigma}^\top D^2 \phi) + f(\mathbf{x})^\top D_{\mathbf{x}} \phi + (V(\mathbf{x}) + cf(\mathbf{x}))^\top D_{\mathbf{y}} \phi \\ - \frac{1}{2} D \phi^\top \hat{K} R^{-1} \hat{K}^\top D \phi = 0, \end{aligned} \quad (11)$$

with the same terminal condition.

Following Kappen [2005a], we define a new value function by

$$\psi(\mathbf{x}, \mathbf{y}, t) = \exp \left( -\frac{\phi(\mathbf{x}, \mathbf{y}, t)}{\lambda} \right),$$

for all  $(\mathbf{x}, \mathbf{y}, t) \in \mathbb{R}^n \times \mathbb{R} \times [0, T]$ , where the constant  $\lambda$  satisfies the condition (3). A calculation shows that (3) implies

$$\hat{\sigma}(t) \hat{\sigma}(t)^\top = \Lambda(t) \sigma \sigma^\top \Lambda(t) = \lambda \hat{K}(t) R^{-1} \hat{K}(t)^\top. \quad (12)$$

Substituting  $\phi = -\lambda \log \psi$  in (11) and using (12) gives a linear PDE for  $\psi$ :

$$\begin{aligned} \psi_t + \frac{1}{2} \text{tr}(\hat{\sigma} \hat{\sigma}^\top D^2 \psi) + f(\mathbf{x})^\top D_{\mathbf{x}} \psi \\ + (V(\mathbf{x}) + cf(\mathbf{x}))^\top D_{\mathbf{y}} \psi = 0 \\ \psi(\mathbf{x}, \mathbf{y}, T) = \exp \left( -\frac{1}{\lambda} \Phi(\mathbf{x}, \mathbf{y}) \right). \end{aligned} \quad (13)$$

What we have shown is that the condition (3) is sufficient to obtain a linear HJB equation (11) for the case of generalized costs, i.e. path integral control is applicable to problems with generalized cost functions provided that (3) holds.

### 3.3 Implementation with implicit sampling

Upon solving (11) or (13) locally around  $(x_t, y_t) = (\mathbf{x}, \mathbf{y})$  at time  $t$ , an optimal control at time  $t$  can be determined by

$$u_t^* = -R^{-1} \hat{K}^\top D \phi(\mathbf{x}, \mathbf{y}, t).$$

Instead of solving (13) with a grid-based scheme, we use the Feynman-Kac formula (e.g. Chorin and Hald [2013]):

$$\psi(\mathbf{x}, \mathbf{y}, t) = \mathbb{E} \left[ \exp \left( -\frac{1}{\lambda} \Phi(\tilde{x}_T, \tilde{y}_T) \right) \right], \quad (14)$$

where the expectation is taken over the stochastic processes  $\{\tilde{x}_s\}_{0 \leq s \leq T}$  and  $\{\tilde{y}_s\}_{0 \leq s \leq T}$  driven by

$$\begin{aligned} d\tilde{x}_s &= f(s, \tilde{x}_s) ds + \sigma dW_s \\ d\tilde{y}_s &= [V(s, \tilde{x}_s) + c(s)f(s, \tilde{x}_s)] ds + c(s) \sigma dW_s \\ (\tilde{x}_t, \tilde{y}_t) &= (\mathbf{x}, \mathbf{y}). \end{aligned} \quad (15)$$

Note that the Brownian motion in the dynamics of  $\tilde{y}$  is the same as that in the dynamics of  $\tilde{x}$ . The Feynman-Kac formula holds because the HJB equation (13) is linear and parabolic. We use (14) to locally evaluate  $\psi$  at any  $(\mathbf{x}, \mathbf{y}, t)$  without a grid (which is impractical in high dimensions).

We first approximate the Feynman-Kac formula, and discretize the time interval  $[0, T]$  with  $\{t_i\}_{i=0}^M$ , where  $t_i = i\Delta t$  and  $\Delta t := \frac{T}{M}$ . Let  $\{\mathbf{x}_i\}_{i=j}^M$  and  $\{\mathbf{y}_i\}_{i=j}^M$  be the discretized trajectories (15) of  $\tilde{x}_s$  and  $\tilde{y}_s$  for  $s \in [t_j, T]$ , respectively, starting from  $(\mathbf{x}_j, \mathbf{y}_j) = (\mathbf{x}, \mathbf{y})$ . Recall that the Brownian motion in the dynamics of  $\tilde{y}$  is the same as that in the dynamics of  $\tilde{x}$ . Therefore, the uncertainty in the path  $\{\mathbf{y}_i\}_{i=j}^M$  is determined by the uncertainty in the path  $\{\mathbf{x}_i\}_{i=j}^M$  and the probability distribution of the path  $\{\mathbf{x}_i\}_{i=j}^M$  defines the probability of the paths  $\{\mathbf{x}_i\}_{i=j}^M$  and  $\{\mathbf{y}_i\}_{i=j}^M$ . We can thus use

$$\begin{aligned} \psi(\mathbf{x}, \mathbf{y}, t_j) &\approx \int d\mathbf{x}_{j+1} \dots \int d\mathbf{x}_M p(\mathbf{x}_{j+1}, \dots, \mathbf{x}_M) \\ &\times \exp \left( -\frac{1}{\lambda} \Phi(\mathbf{x}_M, \mathbf{y}_M) \right). \end{aligned} \quad (16)$$

to approximate (14). When computing  $\mathbf{y}_M$ , we can use the fact that  $\tilde{y}$  satisfies (15) to find that

$$\mathbf{y}_M = \mathbf{y}_j + \sum_{i=j+1}^M V(t_i, \mathbf{x}_i) \Delta t + \sum_{i=j+1}^M c(t_i) (\mathbf{x}_i - \mathbf{x}_{i-1}), \quad (17)$$

converges to  $\tilde{y}_T$  of the second equation in (15) as  $\Delta t \rightarrow 0$ .

To evaluate the discretized path integral (16) we use MC sampling. For example, we can generate  $Q$  trajectories  $\{(\mathbf{x}_i^{(q)}, \mathbf{y}_i^{(q)})\}_{i=j}^M$  of (15) starting from  $(\mathbf{x}_j^{(q)}, \mathbf{y}_j^{(q)}) = (\mathbf{x}, \mathbf{y})$ ,  $q = 1, \dots, Q$ . The MC approximation of (16) then becomes

$$\psi(\mathbf{x}, \mathbf{y}, t_j) \approx \frac{1}{Q} \sum_{q=1}^Q \exp \left( -\frac{1}{\lambda} \Phi(\mathbf{x}_M^{(q)}, \mathbf{y}_M^{(q)}) \right). \quad (18)$$

As the number of samples  $Q$  goes to infinity, the right-hand side converges weakly to the value function, and an optimal control can be synthesized as

$$u_{t_j}^* = -R^{-1} \hat{K}(t_j)^\top D \phi(\mathbf{x}, \mathbf{y}, t_j),$$

where  $D\phi(\mathbf{x}, \mathbf{y}, t_j)$  is computed via numerical differentiation (e.g. forward or centered differences). In practice, we cannot use ‘‘infinitely’’ many samples. In fact we may only be able to generate a few ( $O(1000)$ ) samples. In this case, this ‘‘standard MC scheme’’ can fail, in particular if the running cost  $b$  has deep wells (Kappen [2005a], Theodorou et al. [2010], Morzfeld [2013]). Deep but thin wells in  $V$  imply that many trajectories of (15) end up where  $V$  is large and thus contribute little to the approximation (18) of  $\psi$ . This pitfall can be overcome if one guides the samples to remain where the running cost  $V$  is small.

Here, we achieve this guiding effect via implicit sampling, which takes the running cost into account when generating the samples (Chorin and Tu [2009], Chorin et al. [2010], Morzfeld et al. [2012], Morzfeld and Chorin [2012], Atkins et al. [2013], Morzfeld [2013]). To use implicit sampling, we first substitute  $p(\mathbf{x}_{j+1}, \dots, \mathbf{x}_M)$  in the path integral formula (16)

$$\begin{aligned} p(\mathbf{x}_{j+1}, \dots, \mathbf{x}_M) &= \prod_{i=j+1}^M p(\Delta \mathbf{x}_i) \\ &= (2\pi \det(\sigma \sigma^\top \Delta t))^{-(M-j)/2} \\ &\quad \times \exp\left(-\frac{1}{2} \sum_{i=j+1}^M \mathbf{q}_i^\top (\sigma \sigma^\top \Delta t)^{-1} \mathbf{q}_i\right), \end{aligned}$$

where  $\mathbf{q}_i := \Delta \mathbf{x}_i - f(t_{i-1}, \mathbf{x}_{i-1}) \Delta t$  and

$$\Delta \mathbf{x}_i := \mathbf{x}_i - \mathbf{x}_{i-1} \sim \mathcal{N}(f(t_{i-1}, \mathbf{x}_{i-1}) \Delta t, \sigma \sigma^\top \Delta t). \quad (19)$$

We can then rewrite (16) as

$$\begin{aligned} \psi(\mathbf{x}, \mathbf{y}, t_j) &\approx (2\pi \det(\sigma \sigma^\top \Delta t))^{-(M-j)/2} \\ &\quad \int d\mathbf{x}_{j+1} \cdots \int d\mathbf{x}_M \exp(-F(\mathbf{x})), \end{aligned}$$

where  $\mathbf{x} := (\mathbf{x}_{j+1}, \dots, \mathbf{x}_M) \in \mathbb{R}^{n(M-j)}$  and

$$F(\mathbf{x}) = \frac{1}{\lambda} \Phi(\mathbf{x}_M, \mathbf{y}_M) + \frac{1}{2} \sum_{i=j+1}^M [\mathbf{q}_i^\top (\sigma \sigma^\top \Delta t)^{-1} \mathbf{q}_i]$$

and  $\mathbf{y}_M$  is given by (17). Note that the running cost  $V$  is included in  $F$ , i.e.  $F$  contains information about where  $V$  is large and where it is small.

The high-probability samples (those that correspond to a small running cost) are in the neighborhood of where  $F$  is small, i.e. in the neighborhood of the minimizer

$$\mu := \arg \min_{\mathbf{x}} F(\mathbf{x}).$$

We can generate samples in this neighborhood by mapping the high probability region of a ‘‘reference variable’’  $\xi$  to this neighborhood. Here, we choose a Gaussian reference variable  $\xi \sim \mathcal{N}(0, \mathbf{I}_{n(M-j)})$ , and a linear mapping

$$\mathbf{x} = \mu + L^{-1} \xi, \quad (20)$$

where  $L$  is a Cholesky factor of the Hessian  $H = LL^\top$  of  $F$  evaluated at the minimizer  $\mu$ .

To see why (20) maps the high probability region of  $\xi$  to the neighborhood of  $\mu$ , note that (20) implies that

$$\tilde{F}(\mathbf{x}) - \zeta = \frac{1}{2} \xi^\top \xi, \quad (21)$$

where  $\zeta := \min_{\mathbf{x}} F(\mathbf{x})$  and where

$$\tilde{F}(\mathbf{x}) = \zeta + \frac{1}{2} (\mathbf{x} - \mu)^\top H (\mathbf{x} - \mu)$$

is the Taylor expansion to order 2 of  $F$ . High-probability samples of  $\xi$  are in the neighborhood of the origin, and hence, the right hand side of (21) is small with high probability. Accordingly, the left hand side of (21) is also small with high probability and, therefore, the solutions of (21) are close to the minimizer  $\mu$  of  $\tilde{F}$ , which is also the minimizer of  $F$ .

The sampling equation (20) defines an invertible change of variables from  $\mathbf{x}$  to  $\xi$ , which can be used to write (16) in terms of the reference variable  $\xi$

$$\begin{aligned} \psi(\mathbf{x}, \mathbf{y}, t_j) &\approx (2\pi \det(\sigma \sigma^\top \Delta t))^{-\frac{M-j}{2}} \int d\xi_1 \cdots \int d\xi_{n(M-j)} \\ &\quad \times \exp\left(-\zeta + \tilde{F}(\mathbf{x}(\xi)) - F(\mathbf{x}(\xi)) - \frac{1}{2} \xi^\top \xi\right) \det(J), \end{aligned}$$

where  $J = \partial \mathbf{x} / \partial \xi = L^{-1}$ . Since  $\xi \sim \mathcal{N}(0, \mathbf{I}_{n(M-j)})$ , we may also write

$$\psi(\mathbf{x}, \mathbf{y}, t_j) \approx \frac{\mathbb{E}_\xi[\exp(-\zeta + \tilde{F}(\mathbf{x}) - F(\mathbf{x}))]}{(\det(\sigma \sigma^\top \Delta t))^{\frac{M-j}{2}} \det(L)}.$$

Our implicit sampling-based path integral algorithm can be summarized in three steps:

- (1) Generate samples,  $\xi^{(q)}$ ,  $q = 1, \dots, Q$ , from  $\xi \sim \mathcal{N}(0, \mathbf{I}_{n(M-j)})$ ;
- (2) Transform the samples through the mechanism (20), i.e.,  $\mathbf{x}^{(q)} = \mu + L^{-1} \xi^{(q)}$ ;
- (3) Evaluate the value function  $\psi$  at  $(\mathbf{x}, \mathbf{y}, t_j)$  as

$$\psi(\mathbf{x}, \mathbf{y}, t_j) \approx \frac{1}{Q} \sum_{q=1}^Q \frac{\exp(-\zeta + \tilde{F}(\mathbf{x}^{(q)}) - F(\mathbf{x}^{(q)}))}{(\det(\sigma \sigma^\top \Delta t))^{\frac{M-j}{2}} \det(L)}.$$

For more detail about implicit sampling in the context of path integral control see Morzfeld [2013].

#### 4. HIERARCHICAL MANAGEMENT FOR STOCHASTIC THERMOSTATICALLY CONTROLLED LOADS

We consider a scenario in which a utility company manages the operation of thermostatically controlled loads (TCLs), such as air conditioners, to minimize payments in the real-time market and the discomfort of the consumers. If the utility controls all of the TCLs by monitoring all of the system states (e.g. indoor temperatures), the synthesis of an optimal control is intractable due to high system dimension.

To overcome the system dimension issue, we propose the hierarchical management framework in Fig. 1. A similar hierarchical load control framework is proposed in Callaway and Hiskens [2011]. We assume that all of the TCLs are air conditioners and that exactly one TCL controls the indoor temperature of a single room. The TCLs are classified into  $n$  types, which differ in their temperature-TCL model characteristics (see section 4.1). The key components of the hierarchical management are the local controllers. Local controller  $i$  determines which subset of type  $i$  TCLs should be turned on at each time  $t \in [0, T]$ . Local controller  $i$  communicates with type  $i$  TCLs to gather the data of the indoor temperatures, and then ranks the TCLs from the highest to lowest discomfort level (the precise definition of the discomfort level is given Section 4.2). Each local controller also reports the average indoor temperature to the central controller.

The central controller, which communicates only with the local controllers, computes each TCL group’s optimal power consumption by considering the average temperature-TCL models of all of the groups. Note that the total dimension of the averaged systems is much less than that of all of the temperature-TCL systems. The central controller then delivers group  $i$ ’s optimal power consumption to local controller  $i$  for  $i = 1, \dots, n$ .

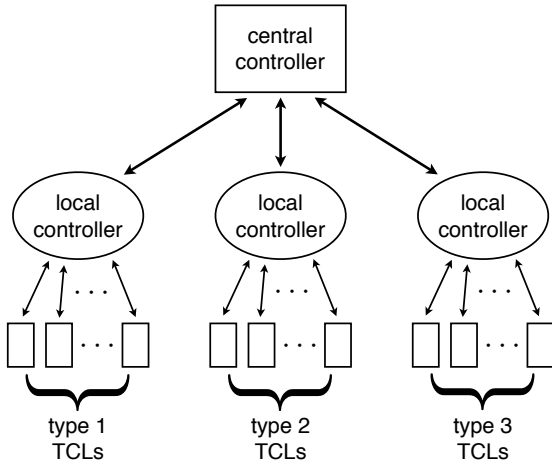


Fig. 1. Hierarchical control for three types of TCLs.

After receiving the optimal power consumption level, local controller  $i$  determines the number  $\mathcal{O}^*$  of TCLs that should be turned on by dividing the optimal level by one TCL's nominal power consumption. The local controller changes the operation of the TCL with the highest rank (the one with the highest discomfort level): i.e., if the TCL is off, the local controller turns it on. The local controller then considers the TCL with the second highest rank, and so on. It stops making changes once the number of TCLs that are on is equal to  $\mathcal{O}^*$ .

We consider the central controller's problem of determining the optimal power consumptions of all of the TCL groups. This stochastic optimal control problem is solved by the generalized path integral method with implicit sampling.

#### 4.1 Stochastic indoor temperature-TCL Model

Let  $\Theta_t^{i,j}$  be the indoor air temperatures at time  $t$  that are controlled by TCL  $j$  of type  $i$  for  $j = 1, \dots, N_i$ , where  $N_i$  is the number of type  $i$  TCLs. The equivalent thermal parameter (ETP) model suggests that the dynamics of the temperatures depend on the conductance  $R_{i,j}$  between the outdoor air and indoor air and the conductance  $C_{i,j}$  of the indoor air and the thermal mass (Sonderegger [1978]). We assume that TCLs of the same type have the same thermal parameters: i.e.,  $R_i := R_{i,j}$  and  $C_i := C_{i,j}$  for  $j = 1, \dots, N_i$ . Let  $\Theta_t^i$  be the average indoor air temperature at time  $t$ , i.e.,  $\Theta_t^i := \frac{1}{N_i} \sum_{j=1}^{N_i} \Theta_t^{i,j}$ . We consider the following stochastic model for the average temperatures:

$$d\Theta_t^i = \left[ \alpha_i (\Theta_t^{O,i} - \Theta_t^i) - \kappa_i \frac{u_t^i}{N_i} \right] dt + \sigma_i dW_t^i \quad (22)$$

where  $\alpha_i = R_i/C_i$ . Here,  $u_t^i$  denotes the total power consumption of the type  $i$  TCLs and  $\Theta_t^{O,i}$  denotes the (day-ahead) forecast of the average outdoor air temperature at time  $t$ . We use the forecast shown in Fig. 2 for our simulations. The effect of the forecast error is modeled by the stochastic term  $\sigma_i dW_t^i$ .

Let  $x_t^i := \Theta_t^i$  for  $i = 1, \dots, n$ ,  $u_t := (u_t^1, \dots, u_t^n)$ ,  $W_t := (W_t^1, \dots, W_t^n)$ , and let  $K$  and  $\sigma$  be  $n \times n$  diagonal matrices whose  $i$ th diagonal entries are  $-\kappa_i/N_i$  and  $\sigma_i$ , respectively. With this notation, we can compactly write the stochastic temperature-TCL model for all types as

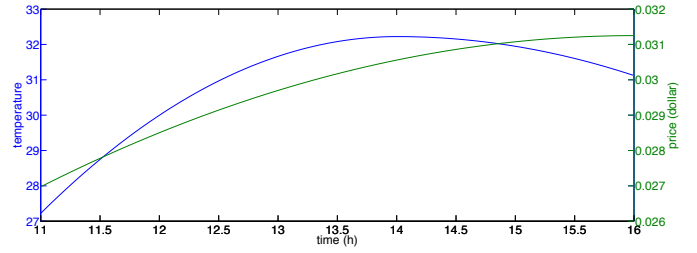


Fig. 2. A forecast of outdoor air temperature,  $\Theta_t^O$  (blue), and an energy price profile,  $p(t)$ , in the real-time market (red).

$$dx_t = [f(t, x_t) + K u_t] dt + \sigma dW_t, \quad (23)$$

where

$$f_i(t, x) := \alpha_i (\Theta_t^{O,i} - x^i)$$

for  $i = 1, \dots, n$ . The central controller determines the total power consumption vector  $u$  using this stochastic temperature-TCL model to achieve the objective discussed below.

#### 4.2 Control objectives

A control objective is to keep the discomfort level small. The discomfort level should be small if the average indoor temperatures are within a given temperature range,  $[\underline{\Theta}, \bar{\Theta}]$ . The discomfort level increases significantly as the indoor temperature drops below  $\underline{\Theta}$  or increases above  $\bar{\Theta}$ . To model this characteristic of the discomfort level, we define

$$\bar{b}(x_t) := \sum_{i=1}^n N_i b_i(x_t),$$

where

$$b_i(x_t) := \eta_1 [\exp(\eta_2(x_t^i - \bar{\Theta})) + \exp(\eta_2(\underline{\Theta} - x_t^i))]$$

for some positive constants  $\eta_1$  and  $\eta_2$ .

Another control objective is to minimize the cost for real-time balancing of the supply and demand. Suppose that the day-ahead energy purchases are sufficiently small and therefore any power supplied to the TCLs must be purchased in the real-time market. The balancing cost in the real-time market at time  $t$  is computed as  $p(t)\mathbf{1}u_t$ , where  $p(t)$  is the unit price of power in kW at time  $t$  (see Fig. 2) in the real-time market and  $\mathbf{1}$  is a 1 by  $n$  vector whose elements are all 1's.

The central controller can determine an optimal power consumption strategy for each TCL group by solving the stochastic optimal control problem:

$$\min_{u \in \mathcal{U}} \mathbb{E} \left[ \int_0^T \bar{b}(x_t) + p(t)\mathbf{1}u_t + \frac{1}{2} u_t^\top R u_t dt \right] \quad (24)$$

subject to (23).

Note that this problem cannot be solved with the path integral method as described in Section 2 due to the term  $p(t)\mathbf{1}u_t$ , which is linear in control. However, we can solve this problem with our generalized formulation of path integral control.

Specifically, we use the stochastic temperature-TCL model (23) and the fact that  $\mathbb{E}[\int_0^T p(t)\mathbf{1}K^{-1}\sigma dW_t] = 0$  to rewrite the objective of (24) as

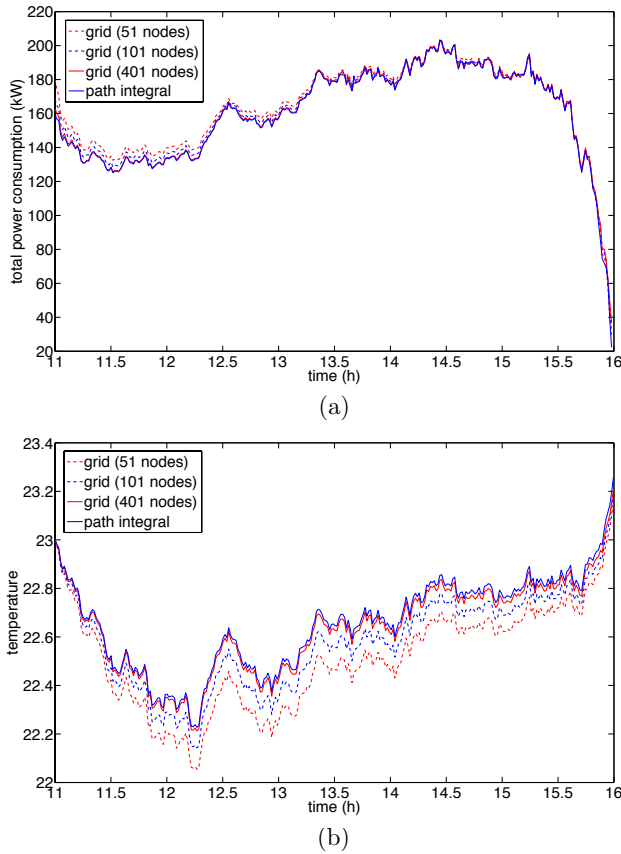


Fig. 3. Comparison of the grid-based method and the path integral-based method: (a) computed optimal control and (b) corresponding state trajectory.

$$\min_{u \in \mathbb{U}} \mathbb{E} \left[ \int_0^T \bar{b}(x_t) - p(t) \mathbf{1} K^{-1} f(t, x_t) dt + \int_0^T p(t) \mathbf{1} K^{-1} dx_t + \frac{1}{2} \int_0^T u_t^\top R u_t dt \right].$$

Let  $V(t, \mathbf{x}) := \bar{b}(\mathbf{x}) - p(t) \mathbf{1} K^{-1} f(t, \mathbf{x})$  and  $c(t) := p(t) \mathbf{1} K^{-1}$ . We introduce a new state variable driven by the following SDE:

$$\begin{aligned} dy_t &= [V(t, x_t) + c(t)(f(t, x_t) + K u_t)] dt + c(t) \sigma dW_t \\ &= [\bar{b}(x_t) + c(t) K u_t] dt + c(t) \sigma dW_t \end{aligned} \quad (25)$$

with  $y_0 = 0$ . In augmented state space, we obtain a stochastic optimal control problem with cost function

$$\min_{u \in \mathbb{U}} \mathbb{E} \left[ y_T + \frac{1}{2} \int_0^T u_t^\top R u_t dt \right]$$

subject to (23) and (25).

We apply the generalized path integral method described in Section 3.3 to solve this problem.

#### 4.3 Numerical tests

*Single TCL type* We first consider the case in which all of the TCLs are of the same type. The grid-based method is applicable to this simple example so that we can compare results obtained via the grid-based method to path integral control. We set  $N_1 = 100$ ,  $\alpha_1 = 0.4834$ ,  $\kappa_1 = 2.5$ ,  $\sigma_1 = 0.2$ ,

$\eta_1 = 1$ ,  $\eta_2 = 5$ ,  $R = 4.6875 \times 10^{-2}$ ,  $\underline{\Theta} = 18$ ,  $\bar{\Theta} = 22$  and  $\Theta_0 = 23$ .

For the path integral method, we use 300 nodes for the time discretization of the time interval [11h, 16h], and 5 samples generated via implicit sampling. For the grid-based method, we use a varying number of nodes (51, 101 and 401) to discretize the state space. The varying number of nodes is used to study the convergence of the grid-based method as the discretization is refined. Both methods lead to a control that induces overcooling before 12pm when the energy price is low even though the outdoor temperature is not high during this period.

Fig. 3 indicates that the optimal control and corresponding state trajectory obtained by the grid-based method approach those obtained by the path integral method as the number of nodes increases. In fact, The difference between the indoor temperature with the optimal control obtained by the path integral method and that with the optimal control obtained by the grid method (with 401 nodes) is less than 1%. This observation suggests that the path integral method is accurate, i.e., the local solution of the HJB equation we obtain via implicit sampling is the desired viscosity solution because the grid-based solution converges to the viscosity solution as the discretization is refined (e.g. Sethian [1999], Osher and Fedkiw [2002] and the references therein).

*Six types of TCLs* We now consider a more realistic scenario with six types of TCLs. The dimension of this problem is large enough to make the grid-based approach impractical. We set  $\alpha = (0.4834, 0.6043, 0.7251, 0.8460, 0.9669, 1.0877)$  and  $\bar{\Theta} = 21.5$ ; all other parameters are as above. We use 100 nodes for the time discretization and  $5^6 = 15625$  samples generated by implicit sampling because using 5 samples gives a good result in the case of single TCL type.

We observe that as  $\alpha_i$  increases, the heat conduction from the outside to the inside increases. Because we assume that the outdoor temperature is higher than the indoor temperature (see Fig. 2), a TCL in a room with a higher  $\alpha_i$  consumes more power to reduce the discomfort level. As expected, the optimal power consumption of the type 6 TCLs (those with the highest  $\alpha$ ) is the highest, and that of the type 1 TCLs (those with the lowest  $\alpha$ ) is the lowest (see Fig. 3 (a)). This is in line with what we intuitively expect from an optimal control.

## 5. CONCLUSIONS AND FUTURE WORK

We generalize the path integral-based method for stochastic optimal control to handle a more general class of cost functions, by introducing a new state. Our generalization makes path integral control more broadly applicable, in particular to applications in engineering, economics and finance. Furthermore, our memory efficient methodology is applicable to problems where most current techniques fail, because it does not require a global grid for discretizing the domain of the HJB equation.

In the future, we plan to relax the condition on the noise covariance and control input matrices. Another interesting



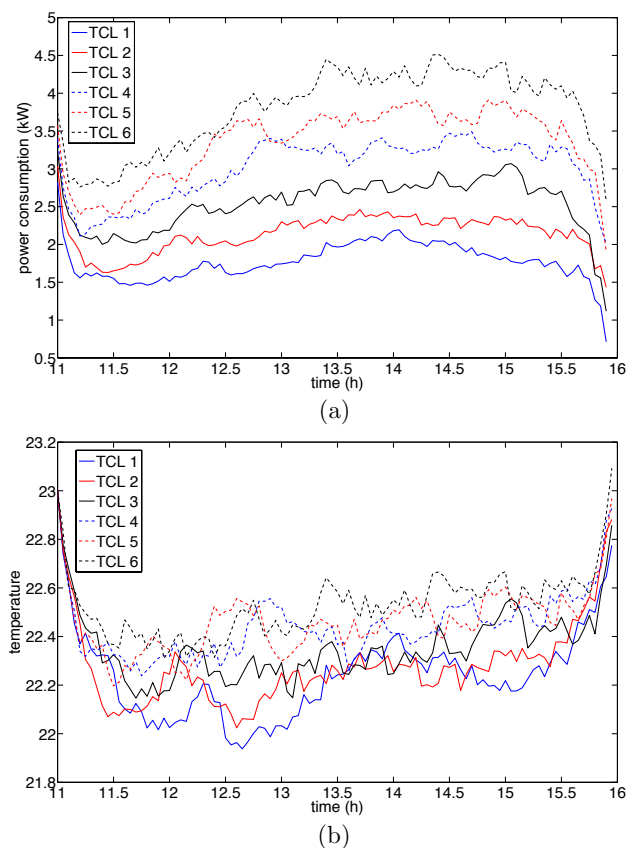


Fig. 4. (a) Computed optimal control and (b) corresponding state trajectory.

direction would be to develop the path integral method for differential games.

#### ACKNOWLEDGEMENTS

The authors would like to thank Professor Lawrence C. Evans for advice on the idea of introducing a new state variable and Professor Duncan S. Callaway for helpful discussions on direct load control.

#### REFERENCES

R. N. Anderson, A. Boulanger, W. B. Powell, and W. Scott. Adaptive stochastic control for the smart grid. *Proceedings of the IEEE*, 99(6):1098–1115, 2011.

E. Atkins, M. Morzfeld, and A. J. Chorin. Implicit particle methods and their connection with variational data assimilation. *Monthly Weather Review*, 141:1786–1803, 2013.

R. Bellman. Dynamic programming and Lagrange multipliers. *Proceedings of the National Academy of Sciences*, 42(10):767–769, 1956.

D. S. Callaway and I. A. Hiskens. Achieving controllability of electric loads. *Proceedings of the IEEE*, 99(1):184–199, 2011.

A. J. Chorin and O. H. Hald. *Stochastic Tools in Mathematics and Science*. Springer, New York, third edition, 2013.

A. J. Chorin and X. Tu. Implicit sampling for particle filters. *Proceedings of the National Academy of Sciences*, 106(41):17249–17254, 2009.

A. J. Chorin, M. Morzfeld, and X. Tu. Implicit particle filters for data assimilation. *Comm. Appl. Math. Comp.*, 5(2):221–240, 2010.

W. H. Fleming and H. M. Soner. *Controlled Markov Processes and Viscosity Solutions*. Springer, 2nd edition, 2005.

B. Holmstrom and P. Milgrom. Aggregation and linear in the provision of intertemporal incentives. *Econometrica*, 55(2):303–328, 1987.

H. J. Kappen. Linear theory for control of nonlinear stochastic systems. *Physical Review Letters*, 95:200201, 2005a.

H. J. Kappen. Path integrals and symmetry breaking for optimal control theory. *Journal of Statistical Mechanics: Theory and Experiment*, 11:11011, 2005b.

W. M. McEneaney and L. J. Klueberg. Convergence rate for a curse-of-dimensionality-free method for a class of HJB PDEs. *SIAM Journal on Control and Optimization*, 48(5):3052–3079, 2009.

W. M. McEneaney, A. Deshpande, and S. Gaubert. Curse-of-complexity attenuation in the curse-of-dimensionality-free method for HJB PDEs. In *Proceedings of 2008 American Control Conference*, pages 4684–4690, 2008.

M. Morzfeld. Implicit sampling for path integral control, Monte Carlo localization and online SLAM. *in review*, 2013.

M. Morzfeld and A. J. Chorin. Implicit particle filtering for models with partial noise, and an application to geomagnetic data assimilation. *Nonlinear Processes in Geophysics*, 19:365–382, 2012.

M. Morzfeld, X. Tu, E. Atkins, and A. J. Chorin. A random map implementation of implicit filters. *Journal of Computational Physics*, 231:2049–2066, 2012.

S. Osher and R. Fedkiw. *Level Set Methods and Dynamic Implicit Surfaces*. Springer, 2002.

H. Ou-Yang. Optimal contracts in a continuous-time delegated portfolio management problem. *The Review of Financial Studies*, 16(1):173–208, 2003.

J. A. Sethian. *Level Set Methods and Fast Marching Methods: Evolving Interfaces in Computational Geometry, Fluid Mechanics, Computer Vision, and Materials Science*. Cambridge University Press, 2nd edition, 1999.

R. C. Sonderegger. *Dynamic Models of House Heating Based on Equivalent Thermal Parameters*. PhD thesis, Princeton University, 1978.

E. Theodorou, F. Stulp, J. Buchli, and S. Schaal. An iterative path integral stochastic optimal control approach for learning robotic tasks. In *Proceedings of the 18th World Congress of the International Federation of Automatic Control*, 2011.

E. A. Theodorou, J. Buchli, and S. Schaal. A generalized path integral control approach to reinforcement learning. *Journal of Machine Learning Research*, 11:3137–3181, 2010.

E. Todorov. Efficient computation of optimal actions. *Proceedings of the National Academy of Sciences*, 106(28):11478–11483, 2009.

I. Yang, D. S. Callaway, and C. J. Tomlin. Dynamic contracts with partial observations: application to indirect load control. In *Proceedings of 2014 American Control Conference*, Portland, OR, 2014.